

# On the Effective Charge of Hydrophobic Polyelectrolytes

A. Chepelianskii <sup>(a)</sup>, F. Mohammad-Rafiee <sup>(b,c)</sup>, E. Trizac <sup>(d)</sup> and E. Raphaël <sup>(c)</sup>

<sup>(a)</sup> *Laboratoire de Physique des Solides, UMR CNRS 8502,*

*Bât. 510, Université Paris-Sud, 91405 Orsay, France*

<sup>(b)</sup> *Institute for Advanced Studies in Basic Sciences (IASBS), Zanjan 45195, P.O. Box 45195-1159, Iran.*

<sup>(c)</sup> *Laboratoire Physico-Chimie Théorique, UMR CNRS Gulliver 7083,*

*ESPCI, 10 rue Vauquelin, 75005 Paris, France and*

<sup>(d)</sup> *Université Paris-Sud, LPTMS, UMR CNRS 8626, 91405 Orsay, France*

(Dated: April 24, 2008)

In this paper we analyze the behavior of hydrophobic polyelectrolytes. It has been proposed that this system adopts a pearl-necklace structure reminiscent of the Rayleigh instability of a charged droplet. Using a Poisson-Boltzmann approach, we calculate the counterion distribution around a given pearl assuming the latter to be penetrable for the counterions. This allows us to calculate the effective electric charge of the pearl as a function of the chemical charge. Our predictions are in good agreement with the recent experimental measurements of the effective charge by Essafi *et al.* (Europhys. Lett. **71**, 938 (2005)). Our results allow to understand the large deviation from the Manning law observed in these experiments.

PACS numbers: 82.35.Rs, 83.80.Rs, 61.25.Hq, 82.45.Gj

## INTRODUCTION

The study of polyelectrolytes has attracted an increased attention in the scientific community over the last decades. This interest is motivated by technological applications including viscosity modifiers, or leak protectors and by the hope that advances in this domain will allow to unravel the structure of complex biological macromolecules. In these systems, the Coulomb interactions leads to many remarkable and counterintuitive phenomena [1, 2, 3, 4, 5]. A celebrated example is the Manning-Oosawa counterion condensation. In his classical work [1], Manning showed that a charged rod-like polymer can create such a strong attractive force on its counterions, that a finite fraction condenses onto the polymer backbone. This condensation-phenomenon was also described by Oosawa within a two state model [2]. It leads to an effective decrease of the polymer charge, and the macroscopic properties of the polyelectrolyte, like migration in an electrophoresis experiment, are not determined by its bare charge, but by an effective charge that accounts for the Manning-Oosawa counterion condensation. It is now well-established that counterion condensation is a fundamental phenomenon, and that it occurs in many important systems including DNA in both its double-stranded and single-stranded form [6]. It was predicted in [1] that condensation occurs whenever the average distance  $l$  between co-ions on the polymer backbone is smaller than the Bjerrum length  $\ell_B = q^2 / (4\pi\epsilon\epsilon_0 k_B T)$ , where  $q$  is the co-ion charge,  $k_B T$  the thermal energy and  $\epsilon$  the (relative) dielectric constant of the solvent. This condensation is expected to lead to an average charge density of  $q/\ell_B$  on the polymer backbone. Since the original prediction by Manning, important efforts have been devoted to a description of the Manning-Oosawa condensation within the Poisson-Boltzmann theory and beyond

[7, 8, 9, 10, 11], establishing the influence of salt, the thickness of the condensed counterion layer and the corrections induced by short range correlation.

While the conformation of many polyelectrolytes is well described by the rod-like model, many proteins organize into complex self-assembled structures [12]. A challenging and important topic is the extent to which the structural complexity of biological enzymes can be understood from simple physical models. Polyelectrolytes with an hydrophobic backbone may provide an interesting system, that achieves a certain degree of self-organization while the relevant interactions remain relatively simple. Indeed it has been predicted in a seminal paper by Dobrynin and Rubinstein that hydrophobic polyelectrolytes should fold into an organized pearl-necklace structure where regions of high and low monomer density coexist [13]. Therefore both theoretical and experimental studies of the hydrophobic polyelectrolytes have shown a growing activity in the past few years [4, 5, 14, 15, 16, 17, 18, 19, 20, 21].

The question of the validity of the Manning condensation model for hydrophobic polyelectrolytes has been addressed experimentally by W. Essafi *et al.* [22]. The authors have measured the effective charge fraction of a highly charged hydrophobic polyelectrolyte (poly(styrene)-co-styrene sulphonate) by osmotic pressure and cryoscopy measurements. Their findings, which are recalled on Fig. 4, showed that the measured effective charge is significantly smaller than that predicted by the Manning-Oosawa theory. The aim of the present article is to provide a theoretical explanation of the counterion condensation in this system, where the presence of hydrophobic interactions influences drastically the conformation of the polymer backbone. This problem was first addressed theoretically by Dobrynin, and Rubinstein [17], who determined the phase diagram

of a solution of hydrophobic polyelectrolytes as a function of solvent quality and polymer concentration. However the question of the effective charge was not directly investigated by the authors.

The rest of the paper is organized as follows: In Sec. II the pearl-necklace model is reviewed briefly, while the Poisson-Boltzmann theory of a hydrophobic globule permeable to counterions is performed in Sec. III. The resulting effective charge is analyzed in Sec. IV. Some aspects of the model are discussed in Sec. V and finally, Sec. VI concludes the paper.

## II. REVIEW OF THE PEARL-NECKLACE MODEL

Let us first recall for completeness the pearl-necklace theory of hydrophobic polyelectrolytes (for a more complete review see [21]). The polyelectrolyte solution is parameterized by its degree of polymerization  $N$ , its monomer size  $b$ , the charge fraction along the chain  $f$ , and the reduced temperature  $\tau \equiv 1 - \frac{\Theta}{T}$ , where  $\Theta$  and  $T$  denote the theta temperature of the polyelectrolyte and the temperature of the system, respectively. We note that in a bad solvent, the reduced temperature is negative  $\tau < 0$ . We let  $C$  be the average monomer concentration in the solution.

In a poor solvent, an uncharged polymer forms a globule in order to decrease its surface energy. In a similar way, a drop of water adopts a spherical configuration in a hydrophobic environment.

To estimate the gyration radius  $R_g$  of the polymer, we divide the polymer into smaller units, in such a way that inside each unit the thermal fluctuations dominate and the chain has Gaussian behavior. These units are usually called thermal blobs in the literature and the typical radius of the blobs is denoted by  $\xi_T$ . It can be shown that they contain about  $1/\tau^2$  monomers, and have a typical size of  $\xi_T \simeq b/|\tau|$ . At larger scales, the polymer tends to collapse onto itself in order to minimize its contact surface with the liquid. This can happen by forming a dense packing of thermal blobs. A polymer of polymerization degree  $N$  can be split into  $\tau^2 N$  thermal blobs and the volume occupied by the polymer is proportional to the number of subunits. Therefore one can estimate the gyration radius of the polymer as

$$R_g^3 \simeq \tau^2 N \xi_T^3 \simeq \frac{N b^3}{|\tau|}. \quad (1)$$

The surface energy  $E_S$  associated with this configuration is given by  $k_B T$  times the number of thermal blobs in contact with the solvent. This leads to

$$\frac{E_S}{k_B T} \simeq \frac{\tau^2 R_g^2}{b^2}. \quad (2)$$

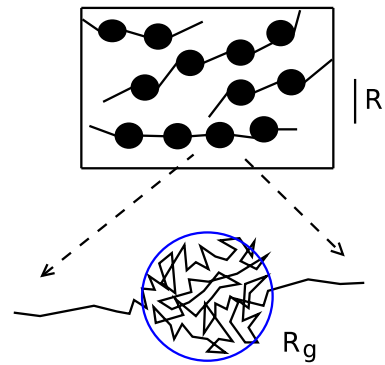


FIG. 1: Schematic drawing of the pearl necklace structure of hydrophobic polyelectrolytes: Inside the blue (gray) circle the polymer backbone, represented by a continuous black line, is wrapped into a dense configuration of typical radius  $R_g$ , that we call pearl or globule in the text. The inset shows on a larger scale, that these pearls are connected by thin polymer strings, thus forming the pearl necklace structure. The average distance between the pearls is  $R$  (black vertical scale line).

Upon charging, the electrostatic repulsion sets in, which results in a change of the globule shape. When the electrostatic repulsion energy becomes larger than the surface energy, the globule splits into several globules of smaller size consisting of  $N_g$  monomers. The typical size of these globules can be found from Eq. (1) with the number of monomers  $N_g$ , which gives

$$R_g^3 \simeq \frac{N_g b^3}{|\tau|}. \quad (3)$$

This behavior is reminiscent of the Rayleigh instability of a charged droplet [23]. In this state, the polyelectrolyte forms a sequence of globules that are connected by strings made of thermal blobs (see Fig. 1). In the literature, this conformation is known as the “pearl-necklace” structure. The presence of counterions will screen the electrostatic repulsion. Therefore it is important to account for their role explicitly in the balance between the surface tension and the electrostatic repulsion that governs the equilibrium structure of the necklace.

For simplicity we assume that the main effect of the counterions is to reduce the charge of the pearls. Indeed, some counterions can be attracted inside the globules due to the attractive electrostatic forces. We assume that the charged monomers of the polyelectrolyte have only one elementary charge  $q$ . In the absence of any counterion condensation, the total electrostatic charge of a globule consisting of  $N_g$  monomers is given by  $q f N_g$ . As long as the counterions penetrate inside the globule, the effective charge of a globule is decreased and is given by  $q f_{eff} N_g$ , where  $f_{eff}$  denotes the effective charge fraction. We can understand this relation by noting that in the presence of counterion condensation the total charge of the pearl is

the chemical charge of the pearl minus the charge of the counterions inside it. Therefore, the electrostatic energy  $E_{el}$  of a pearl can be estimated as

$$\frac{E_{el}}{k_B T} \simeq \frac{\ell_B (f_{eff} N_g)^2}{R_g}, \quad (4)$$

where the Bjerrum length is defined as

$$\ell_B = \frac{q^2}{4\pi\epsilon\epsilon_0 k_B T}, \quad (5)$$

where  $\epsilon$  is the dielectric constant of the medium and  $k_B T$  denotes the thermal fluctuation energy. For example for water at room temperature ( $T = 300$  K,  $\epsilon = 80$ ) the value of the Bjerrum length is  $\ell_B \approx 0.7$  nm. Using the relation between  $R_g$  and the  $N_g$  given in Eq. (3), the electrostatic energy of a pearl is simplified to

$$\frac{E_{el}}{k_B T} \simeq |\tau|^2 f_{eff}^2 \frac{\ell_B R_g^5}{b^6}. \quad (6)$$

In its equilibrium configuration the pearl-necklace tends to balance its electrostatic and surface energies  $E_{el} \simeq E_S$ . Inserting the results of Eq. (2) and Eq. (6) in this equality leads to an expression of the globule radius  $R_g$  as a function of the effective charge fraction  $f_{eff}$ :

$$R_g \simeq b \left( \frac{b}{\ell_B} \right)^{1/3} \frac{1}{f_{eff}^{2/3}}. \quad (7)$$

We stress that this relation between the typical pearl size and the effective charge has been verified experimentally by D. Baigl *et al.* in [24] with an X-ray diffraction technique. This suggests that the hydrophobic polyelectrolytes studied in the experiment of W. Essafi actually formed a pearl necklace structure.

### III. SCREENING OF A GLOBULE IN THE POISSON-BOLTZMANN THEORY

The problem of the effective charge of spherical microion-permeable globules of size  $R_g$  surrounded by their own counterions can be solved in the mean-field approximation using the Poisson-Boltzmann theory. This problem was first studied numerically and analytically by Wall and Berkowitz [25]. It was shown that counterion condensation around such a globule is possible (see e.g. Ref [26] for a general discussion of the condensation phenomenon). In this approach, a charged globule is modelled as a sphere with radius  $R_g$  and a uniform charge distribution inside it. Therefore, the charge density of the globule is given by

$$q\rho_0 \simeq q \frac{f N_g}{R_g^3}, \quad (8)$$

where  $\rho_0$  denotes the mean density of charged monomers that are distributed inside the globule. Using Eq. (3),  $\rho_0$  can be simplified to

$$\rho_0 \simeq \frac{f|\tau|}{b^3}. \quad (9)$$

In the solution, the mean monomer concentration is denoted by  $C$ . As far as the counterions are distributed inside an elementary cell of radius  $R$  (Wigner-Seitz approach), the average concentration of the counterions is given by

$$n_{av} = fC. \quad (10)$$

Using the electro-neutrality condition, one can find a relation between the radius of the elementary cell,  $R$ , and the density of the charged monomers inside the globule as

$$\rho_0 R_g^3 = n_{av} R^3. \quad (11)$$

Assuming the spherical symmetry in the charge distribution, all the quantities such as the electrostatic potential, the counterion concentration, *etc* depend only on the distance  $r$  to the center of the globule. Under the assumption of a Boltzmann-distribution, the concentration profile  $n(r)$  of the counterions is related to the electrostatic potential  $\phi(r)$  as

$$n(r) = n_{av} e^{\frac{q\phi(r)}{k_B T}}. \quad (12)$$

Inserting this expression into the Poisson equation  $\nabla^2 \phi = -\frac{1}{\epsilon\epsilon_0} (q\rho_0(r) - qn(r))$  leads to the well-known Poisson-Boltzmann (PB) equation:

$$\nabla^2 \phi = \frac{1}{r^2} \frac{d}{dr} \left( r^2 \frac{d\phi}{dr} \right) = -\frac{q\rho_0(r)}{\epsilon\epsilon_0} + \frac{qn_{av}}{\epsilon\epsilon_0} e^{\frac{q\phi}{k_B T}}, \quad (13)$$

where  $\rho_0(r)$  is given by

$$\rho_0(r) = \begin{cases} \rho_0 \simeq \frac{f N_g}{R_g^3} & r \leq R_g, \\ 0 & r > R_g. \end{cases} \quad (14)$$

For our system with spherical symmetry in the charge distribution, the electric field is zero at  $r = 0$ . Electroneutrality also demands a vanishing electric field at the boundary  $r = R$ , so that the boundary conditions for the above PB equation read

$$\frac{d\phi(r=0)}{dr} = \frac{d\phi(r=R)}{dr} = 0. \quad (15)$$

In an elementary cell with the average counterion density  $n_{av}$ , the Debye screening length  $\lambda_D$  is given by

$$\frac{1}{\lambda_D^2} = 4\pi\ell_B n_{av}. \quad (16)$$

After defining the reduced electrostatic potential,  $u \equiv q\phi/(k_B T)$ , and  $x \equiv r/\lambda_D$ , PB equation can be written as

$$\frac{d^2 u}{dx^2} + \frac{2}{x} \frac{du}{dx} = e^{u(x)} - A(x), \quad \frac{du(0)}{dx} = \frac{du(X)}{dx} = 0, \quad (17)$$

where  $X$  denotes  $R/\lambda_D$  and  $A(x)$  is defined as

$$A(x) \equiv \frac{\rho_0(x)}{n_{av}}. \quad (18)$$

The radius of the globule in the dimensionless form is denoted by  $x_g \equiv R_g/\lambda_D$ . We will set  $A$  as the value of  $A(x)$  inside the globule:  $A(x) = A$  for  $x \leq x_g$ . Using the aforementioned reduced variables and the cell neutrality condition, Eq. (11), one can find the simple form of  $A$  as

$$A = \frac{\rho_0}{n_{av}} = \left(\frac{X}{x_g}\right)^3 \simeq \frac{|\tau|}{Cb^3}, \quad (19)$$

where in writing the last term, the explicit forms of  $\rho_0$ , Eq. (9), and  $n_{av}$ , Eq. (10), have been used. One can see that  $A$  does not depend on the chemical charge  $f$ .

The fraction of counterions outside the globule,  $P$ , can be found as

$$P = \frac{\int_{r_g}^R n_{av} e^{q\phi(r)/k_B T} r^2 dr}{\int_0^{R_g} \rho_0 r^2 dr} = \frac{\int_{x_g}^X e^u x^2 dx}{\int_0^{x_g} A x^2 dx}, \quad (20)$$

where in writing the last term, the reduced variables and Eq. (19) have been used. Using Eq. (17) and integrating, leads to a simpler form of the above equation as

$$P(x_g, A) = -\frac{3}{x_g A} \frac{du(x_g)}{dx}. \quad (21)$$

As far as the penetrated counterions inside the globule reduce its charge, the effective charge of the globule is proportional to the fraction of counterions outside the globule. Therefore, the effective charge of the globule can be written as

$$f_{eff} = P(x_g, A)f. \quad (22)$$

It has been shown in [25] that the potential  $u(x)$  defined by the boundary problem, Eq. (17), is a decreasing function of  $x$  and the initial value of the potential satisfies  $e^{u(0)} \leq A$ . Physically, this inequality signifies the absence of over-screening (inside the globule  $qn(r) \leq \rho_0$ ) as expected in a mean-field theory [27]. In order to estimate the lower limit of  $e^{u(0)}$ , we re-write Eq. (17) as

$$u(x) = u(0) + \int_0^x \left(y - \frac{y^2}{x}\right) \left[e^{u(y)} - A(y)\right] dy. \quad (23)$$

Since  $u(x)$  is a decreasing function, it may be shown that

$$u(x) = u(0) + \frac{1}{6} \min(x, x_g)^2 \left[e^{u(0)} - A\right], \quad (24)$$

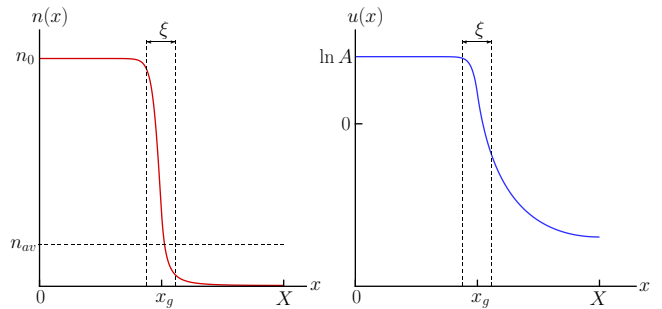


FIG. 2: Typical behavior of counterion charge distribution  $n(x)$  and effective potential  $u(x)$  in the cell. The dimensionless globule size is denoted by  $x_g$  and the cell size is denoted by  $X$ .

where  $\min(x, x_g)$  yields the smaller quantity. After inserting this result in the cell neutrality condition,  $\int_0^X x^2 [e^{u(x)} - A(x)] dx$ , we find that  $e^{u(0)}$  satisfies the following inequality relations:

$$1 - \frac{\ln Z}{Z} \leq \frac{e^{u(0)}}{A} \leq 1, \quad (25)$$

where  $Z$  is defined as  $Z \equiv Ax_g^2/6 > e$ . Therefore, the above chain of inequalities implies that in the limit where  $Ax_g^2 \gg 1$ , we have  $e^{u(0)}/A \rightarrow 1$ .

The behavior of a typical solution  $u(x)$  is displayed in Fig. 2. It confirms that for large values of  $Ax_g^2$ , the counterion concentration at  $x \simeq 0$  is very close to the concentration of charged monomers inside the globule:  $e^{u(x)} \simeq A$ . As the value of  $Ax_g^2$  increases, the size of the neutral region where  $u(x) \approx \ln A$  grows until it becomes of the order of globule size  $x_g$ . Therefore, to keep the system electrically neutral, the counterion concentration must fall down to values below  $n_{av}$  outside the globule.

The transition between these two regions occurs in a narrow layer of thickness  $\xi$  on the boundary of the globule, as shown in Fig. 2. In order to estimate the behavior of  $\xi$  in terms of physical parameters in the problem, it is convenient to write PB equation for  $x \gtrsim x_g$  in the following manner

$$\frac{d^2 u}{dx^2} \left[1 + \frac{2}{x} \frac{du}{dx}\right] = e^{u(x)}. \quad (26)$$

We note that  $d^2 u/dx^2$  and  $du/dx$  are of the order of  $(\ln A)/\xi^2$  and  $(\ln A)/\xi$ , respectively. Putting these values in the above equation, we find

$$\frac{\ln A}{\xi^2} \left[1 + 2 \frac{\xi}{x_g}\right] \simeq A. \quad (27)$$

We assume that we are in the regime where  $\xi/x_g \ll 1$ . Therefore,  $\xi$  scales

$$\frac{\ln A}{\xi^2} \simeq A \implies \xi \simeq \frac{1}{\sqrt{A}}, \quad (28)$$

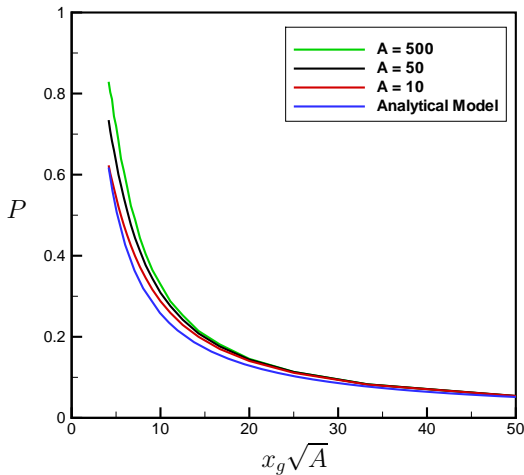


FIG. 3: Dependence of  $P$  on  $x_g\sqrt{A}$  for different values of  $A$ . From top to bottom,  $A = 500, 50, 10$  (green, black, red curves respectively). The bottom (blue) curve is Eq. (29).

where we have neglected the logarithmic dependence on  $A$ . We note that for consistency, the requirement  $\xi \ll x_g$  also implies  $Ax_g^2 \gg 1$ .

We are now in a position to estimate the counterion concentration outside the globule. Using Eq. (21) in the limit of  $Ax_g^2 \gg 1$ , the fraction of counterion outside the globule is found as

$$P(x_g, A) \simeq \frac{1}{x_g A} \frac{u}{\xi} \simeq \frac{6}{\sqrt{2e}} \frac{1}{x_g \sqrt{A}}. \quad (29)$$

The proportionality constant in Eq. (29) is calculated by ignoring the first derivative term  $\frac{1}{x} \frac{du}{dx}$  in Eq. (17). Fig. 3 shows that there is a very good agreement between the exact and the analytical approximation results in the limit of  $Ax_g^2 \gg 1$  ( $\xi \ll x_g$ ). We also see that for a wide range of  $A$  values, our analytical theory gives a good numerical approximation for  $P$  as far as  $P \lesssim 0.4$ . For example for  $A = 500$ , the relative error of our approximation is below 20% in this region. The exact numerical results were obtained using the method described in [25].

#### IV. THE EFFECTIVE CHARGE OF A HYDROPHOBIC POLYELECTROLYTE

In the regime explored experimentally by W. Essafi *et al.* [22], the value of the dimensionless parameter  $A$  can be estimated as follows. For  $|\tau| \simeq 1$ , monomer concentration  $C = 0.1 \text{ Mol L}^{-1}$  and the bond length in the polymer  $b = 0.25 \text{ nm}$ , the expected value of  $A \simeq |\tau|/(Cb^3)$  is  $A \simeq 10^3 \gg 1$ . The value of  $x_g$  depends on both the

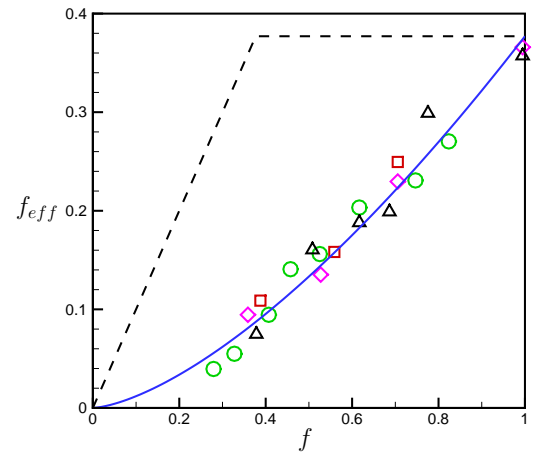


FIG. 4: Effective charge fraction  $f_{eff}$  versus the chemical charge fraction  $f$ . The experimental points were obtained in [22]. The red squares correspond to  $N = 410$ , green circles:  $N = 930$ , purple diamonds:  $N = 1320$ , and black deltas:  $N = 2400$ . The blue solid line corresponds to our theoretical model Eq. (31) with  $\sqrt{b}/(|\tau|^3 \ell_B) = 0.37$ . The dashed line corresponds to Manning's model.

chemical and effective charge fraction,  $f$  and  $f_{eff}$ , as

$$x_g = \frac{R_g}{\lambda_D} \simeq \frac{|\tau|^{1/2}}{A^{1/2}} \left( \frac{\ell_B}{b} \right)^{1/6} \frac{f^{1/2}}{f_{eff}^{2/3}}. \quad (30)$$

Using Eqs. (22), (29), and (30) the effective charge fraction  $f_{eff}$  is found as

$$f_{eff} \simeq \sqrt{\frac{b}{|\tau|^3 \ell_B}} f^{3/2}. \quad (31)$$

This result predicts that the effective charge fraction  $f_{eff}$  is proportional to  $f^{3/2}$ . We note that in this regime the effective charge does not depend on the average monomer concentration  $C$  and depends only on intrinsic properties of the polymer. The scaling law of Eq. (31) and the experimental data of Fig. 4 of [22] are shown in Fig. 4. As one can see, there is a very good agreement between the predicted behavior and the experimental data. We stress that only one free coefficient of order one has been used to adjust the data. Thus, our theory can explain the origin of the difference between the effective charge predicted by the Manning-law recalled on Fig. 4 and that observed in experiments. Furthermore, using Eqs. (3), (7), and (31) the globule radius  $R_g$  and the number of monomers inside the globule  $N_g$  are found as

$$R_g \simeq \frac{|\tau|b}{f}, \quad (32)$$

$$N_g \simeq \frac{|\tau|^4}{f^3}. \quad (33)$$

It is important to mention that in the experiments of [22], only samples with relatively high chemical charge

fraction  $f \geq 0.3$  were prepared, thereby limiting the range where our theory can be checked. This is related to the difficulty to stabilize solutions of hydrophobic polyelectrolytes with low chemical charge because the polyelectrolytes can form a macroscopic phase that is not soluble in the solvent. We expect that the formation of a macroscopic phase can occur if the number of monomers inside a globule  $N_g$  becomes larger than the polymerization degree of the polymer  $N$ . In this case the polymer chains must stick together to form globules of size  $N_g \approx |\tau|^4/f^3 > N$ , which may lead to form an entangled polymer network that is not soluble in the solvent anymore. More detailed theoretical studies are needed on this problem. We note that a detailed analysis of the possible phases and their stability range has been done in [28]. As mentioned above, the dimensionless factors are of order one and if we set  $N = 1000$  this condition for phase separation reads  $f_{eff} < 1/\sqrt{N} \simeq 0.03$ . This result is in a reasonable agreement with the results displayed in Fig. 4. It is worth to mention that in the experiments no point could be obtained below this limit. We also emphasize that in our theory, when a stable pearl-necklace structure forms, the effective charge depends on  $N_g$  and not on polymerization degree  $N$ . This property has been verified in the experiment, where  $N$  has been varied from  $N = 410$  to  $N = 2400$  without apparent change of the measured values of  $f_{eff}$ .

## V. DISCUSSION

In the above treatment, we have assumed that the polyelectrolyte chain in a dilute regime forms a necklace structure in the solvent. Liao *et al.* [29] have studied the necklace formation in polyelectrolyte solutions using both theory and molecular dynamics simulations. They have shown that partially charged chains form necklace-like structures of globules and strings in dilute solutions. For the dilute regime the phase diagram of hydrophobic polyelectrolytes was obtained in [29]. It has been shown that when the effective charge of the chain is larger than a threshold  $\sqrt{b|\tau|/(\ell_B N)}$ , the necklace structure is the dominant feature of the polyelectrolytes in a bad solvent. Using Eq. (31) and the mentioned criterion, we find that for chains consisting of more than  $1/(|\tau|^2 f^3)$  monomers, the necklace-structure is formed in the system. For the experimental condition explained in [22],  $|\tau| \simeq 1$  and  $f > 0.2$ , gives  $1/(|\tau|^2 f^3) \simeq 150$ . All the chains that have been used in the experiment [22] have more than 410 monomers on a chain, which means that our model considering necklace structure for the hydrophobic polyelectrolyte in the solution is reasonable. We note that our approach, does not allow to predict accurately the phase diagram of the polyelectrolyte chains. A consistent minimization of the free energy requires to account correctly for the logarithmic dependence of the counterion entropic

and electrostatic energy as a function of the pearl radius [30]. In our scaling law analysis, it is not possible to follow the mentioned process. The origin of such logarithmic terms can be seen easily by estimating the entropy of the counterions, since the condensed counterions explore only a phase volume of  $R_g^3$  out of the total volume. In our analysis this dependence is ignored because the available phase volume is limited to the size of the Wigner-Seitz cell in a periodic system. Furthermore, the correlation induced effects like the nonmonotonic dependence of the solution osmotic coefficient on the polymer concentration have been observed in computer simulation analysis [29], which cannot be described in our model.

As we explained before, Eq. (31) is based on the validity of Eq. (29). It is justified provided  $P \ll 1$  and our numerical calculations suggest that reasonable agreement is achieved for  $P \lesssim 0.4$  for the experimental value of  $A \simeq 10^3$ . For the parameters used in Fig. 4, the mentioned criterion is always satisfied. Furthermore, by placing the pearls inside neutral Wigner-Seitz cells, we have ignored the effect of the interaction between neighboring pearls on the counterion distribution. However the sharp decrease of the counterion concentration on the boundary of the globule (see Fig. 2) suggests that these interactions should not affect significantly the counterion distribution. We have also ignored the effect of the ions along the strings that connect adjacent pearls. This assumption can be checked by estimating the fraction  $s$  of the charged monomers present inside the pearls. It can be shown that

$$s \simeq \frac{1}{1 + f_{eff} \sqrt{\frac{\ell_B}{|\tau|^3 b}}} \simeq \frac{1}{1 + f_{eff}}, \quad (34)$$

where we have assumed that both the parameter  $\sqrt{\frac{\ell_B}{|\tau|^3 b}}$  and intermediate scaling constants are of order one. These assumptions are consistent with the parameters used in Fig. 4. Our theory holds as long as  $s \simeq 1$ , that is when the effective charge  $f_{eff}$  is small. While this is clearly the case in the range of small chemical charge  $f$ , the contribution of the strings may become important when  $f \simeq 1$ . Physically we expect that around the strings, the counterions will follow the usual Manning-condensation behavior. Therefore, the effect of the strings will be mainly to keep the effective charge  $f_{eff}$  below the Manning limit  $b/\ell_B$ . In Fig. 4, the effective charge reaches this limit only at  $f \simeq 1$ ; as a result the effect of the strings is not visible and our prediction holds even up to  $f \simeq 1$ .

Finally we have not taken into account additional counterion condensation outside the permeable globule. A popular criterion for counterion condensation in this setting, was proposed by Alexander *et al.* [31]. The renormalized charge  $qZ^*$  of an impermeable globule of chemical charge  $qZ$ , is determined from a linearization of the PB equation that ensures the best possible matching

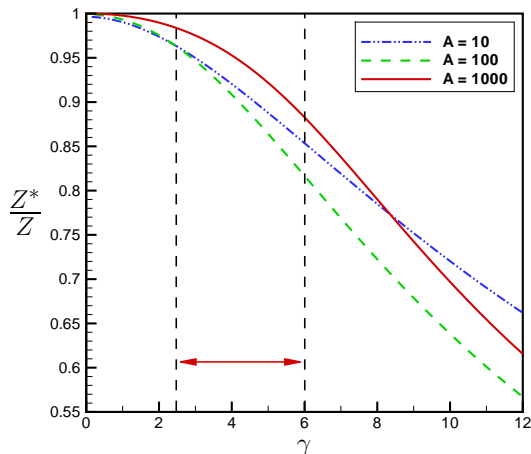


FIG. 5: Ratio between the Alexander charge of the globule  $qZ^*$  and the total charge inside the globule  $qZ = qf_{eff}N_g$  as a function of  $\gamma = Z\ell_B/R_g$  for different values of  $A$ . ( $A \approx 10^3$  in the experimental conditions). The red arrow indicates the parameter range explored experimentally by Essafi *et al.* estimated from Eq. (35).

between the exact and linearized solution at the boundary of the Wigner-Seitz cell. The dependence of the condensed fraction  $Z^*/Z$  on the system parameters, is governed by the dimensionless parameter  $\gamma = (Z\ell_B)/R_g$ , where  $R_g$  is the globule radius [31, 32]. This parameter can be estimated as follows for the case of our permeable pearl model. The charge fraction  $Z$  of the pearl is given by  $Z = f_{eff}N_g = f_{eff}|\tau|R_g^3/b^3$ , using Eqs. (31) and (32) we find that

$$\gamma = \frac{Z\ell_B}{R_g} \simeq \sqrt{\frac{|\tau|^3\ell_B}{b}} \frac{1}{\sqrt{f}} \simeq \frac{1}{0.37\sqrt{f}} \quad (35)$$

Here we used the numerical value for the coefficient  $\sqrt{|\tau|^3\ell_B/b}$  obtained from the fit to the experimental data in Fig. 4. As a consequence, in the parameter regime explored experimentally by W. Essafi *et al.*:  $f \in (0.2, 1)$ , we expect that  $\gamma$  varies in the interval  $\gamma \in (2.5, 6)$ . We have calculated the ratio  $Z^*/Z$  in this parameter range using the semi-analytical method proposed in [33] and our numerical procedure. The obtained results are presented in Fig. 5, which show that for  $A \simeq 10^3$ , the ratio  $Z^*/Z$  is larger than 0.85 when  $\gamma \leq 6$ . This implies that our expression for the effective charge is not renormalized significantly by condensation outside the globule.

It is interesting to compare our results to the results of [17]. Dobrynin and Rubinstein considered for the first time the problem of counterion-condensation around an hydrophobic polyelectrolyte using a two-state model. They determined the fraction  $P$  by using trial counterion densities of the form  $n(r) = (1 - P)n_{av}\frac{R^3}{R_g^3}$  inside the globule (for  $r < R_g$ ), and  $n(r) = Pn_{av}\frac{R^3}{R^3 - R_g^3}$  in

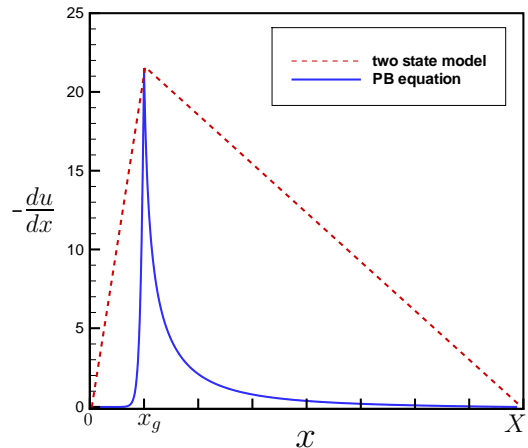


FIG. 6: Typical behavior of the dimensionless electric field  $-\frac{du}{dx}$  using either the two state model (dashed line) or our PB model (solid line). The solid line corresponds to  $x_g = 1$  and  $A = 500$ .

the outer region. This family of density is parameterized only by the parameter  $P$ . Therefore by minimizing the counterion free-energy density functional on this trial set, they could deduce an expression of  $P$  as a function of the system parameters [34]. However for reasonable values of  $|\tau| \left(\frac{b}{\ell_B}\right)^{1/3} \simeq 1$ , and for the experimental value of  $A \simeq 10^3$ , the value of  $f_{eff}$  predicted from the equations of ref. [17] is very close to  $f$  in most of the parameter range in contradiction with the experimental results of [22]. We attribute the difference between our model and the results of [17] to the two state model used to estimate the fraction of dissociated counterions  $P$ . Indeed in the two state model the charge density is constant in the two regions inside and outside the globule. The Poisson equation then implies that in the two-state approximation, the graph of the electric field ( $-\frac{du}{dx}$  in our dimensionless units) as a function of  $x$  has a typical angle shape for all values of  $P$  as illustrated in Fig. 6. In this figure, we have also compared this approximation, to the exact numerical behavior of  $-\frac{du}{dx}$ , for the typical parameters  $A = 500, x_g = 1$ . Since the charged monomers at the center of the globule are neutralized by the counterions, the true electric field distribution takes the form of a narrow peak centered at  $x_g$ . Because of its reduced family of trial functions, the two-state model can not reproduce the true behavior of the electric field. However the determination of the effective charge requires an accurate knowledge of the electric-field in the whole cell. Therefore, we believe that the two state model is not accurate enough for the determination of the effective charge. Indeed it was shown in [35] that at least a three state model is necessary in the case of a permeable droplet.

## VI. CONCLUSIONS

In conclusion, we have developed a theory of counterion condensation around hydrophobic polyelectrolytes. Our theory is based on the pearl-necklace model for the polyelectrolyte backbone. We assumed that the pearls are permeable to the counterions, and use analytic results on the Poisson-Boltzmann equation to establish the fraction of counterions condensed inside the pearls. It allows us to establish a power law dependence of the effective charge  $f_{eff}$  on the chemical charge  $f$  as  $f_{eff} \propto f^{3/2}$ . This prediction is in very good agreement with recent experimental results by W. Essafi *et al.* [22] and explains the large deviation from the Manning law observed in these experiments. While our main results concern the effective charge of hydrophobic polyelectrolytes, the scaling laws that we derived may also apply to other areas of physics and chemistry where the Poisson-Boltzmann equation plays an important role.

## ACKNOWLEDGMENTS

We thank D. Baigl, M. Rubinstein, A. V. Dobrynin, and M. Maleki for fruitful discussions and precious remarks. One of us, A. Chepelianskii, acknowledges the support of Ecole Normale Supérieure de Paris.

- 
- [1] G. S. Manning, *J. Chem. Phys.* **51**, 924 (1969).  
 [2] F. Oosawa, *Polyelectrolytes* (Marcel Dekker, New York, 1971).  
 [3] Y. Kantor, H. Li, and M. Kardar *Phys. Rev. Lett.* **69**, 61 (1992).  
 [4] J.-L. Barrat and J.-F. Joanny, *Adv. Polym. Sci.* **94**, 1 (1996).  
 [5] C. Holm, J.-F. Joanny, K. Kremer, R. R. Netz, P. Reineker, C. Seidel, T. A. Vilgis, and R. G. Winkler, *Adv. Polym. Sci.* **166**, 67 (2004).  
 [6] V. A. Bloomfield, D. M. Crothers and I. Tinoco, *Nucleic Acids Structures, Properties and Functions* (University Science Books, Sausalito, CA, 2000).  
 [7] J. R. Philif and R. A. Wooding, *J. Chem. Phys.* **52**, 953 (1970).  
 [8] B. O'Shaughnessy and Q. Yang, *Phys. Rev. Lett.* **94**, 048302 (2005).  
 [9] E. Trizac and G. Téllez, *Phys. Rev. Lett.* **96**, 038302 (2006).  
 [10] P. Gonzalez-Mozuelos and M. Olvera de la Cruz, *J. Chem. Phys.* **103**, 22 (1995).  
 [11] A. Naji and R. R. Netz, *Phys. Rev. Lett.* **95**, 185703 (2005); *Phys. Rev. E* **73**, 056105 (2006).  
 [12] B. Alberts, D. Bray, A. Johnson, J. Lewis, M. Raff, K. Roberts, and P. Walter, *Essential Cell Biology* (Garland Publishing, New York, 1998).  
 [13] A. V. Dobrynin, M. Rubinstein, and S. P. Obukhov, *Macromolecules* **29**, 2974 (1996).  
 [14] E. Raphael and J.-F. Joanny, *Europhys. Lett.* **13**, 623 (1990).  
 [15] P. G. Higgs and E. Raphael, *J. Phys. I France* **1**, 1(1991).  
 [16] M. D. Carbajal-Tinoco and C. E. Williams, *Europhys. Lett.* **52**, 284 (2000).  
 [17] A. V. Dobrynin and M. Rubinstein, *Macromolecules* **34**, 1964 (2001).  
 [18] M.-J. Lee, M. M. Green, F. Mikes, and H. Morawetz, *Macromolecules* **35**, 4216 (2002).  
 [19] A. Kyriy, G. Gorodyska, S. Minko, W. Jaeger, P. Stepanek, and M. Stamm, *J. Am. Chem. Soc.* **124**, 13454 (2002).  
 [20] H. J. Limbach and C. Holm, *J. Phys. Chem. B* **107**, 8041 (2003).  
 [21] A. V. Dobrynin and M. Rubinstein, *Prog. Polym. Sci.* **30**, 1049 (2005).  
 [22] W. Essafi, F. Lafuma, D. Baigl, and C. E. Williams, *Europhys. Lett.* **71**, 938 (2005).  
 [23] L. Rayleigh, *Philos. Mag.* **14**, 184 (1882).  
 [24] D. Baigl, R. Ober, D. Qu, A. Fery and C. E. Williams, *Europhys. Lett.* **62** 588 (2003).  
 [25] F. T. Wall and J. Berkowitz, *J. Chem. Phys.* **26**, 114 (1957).  
 [26] L. Belloni, *Colloids Surf. A*, 227, **140** (1998).  
 [27] E. Trizac, *Phys. Rev. E* **62**, R1465 (2000).  
 [28] H. Schiessel, and P. Pincus, *Macromolecules* **31**, 7953 (1998).  
 [29] Q. Liao, A. V. Dobrynin, and M. Rubinstein, *Macromolecules* **39**, 1920 (2006).  
 [30] A. V. Dobrynin, and M. Rubinstein, *Macromolecules* **32**, 915 (1999).  
 [31] S. Alexander, P. M. Chaikin, P. Grant, G. J. Morales, P. Pincus, and D. Hone, *J. Chem. Phys.* **80**, 5776 (1984).  
 [32] L. Belloni, M. Drifford, and P. Turq, *Chem. Phys.* **83**, 147 (1984).  
 [33] E. Trizac, L. Bocquet, M. Aubouy, and H. H. von Grunberg, *Langmuir* **19**, 4027 (2003).  
 [34] The final result is given in Eq. (21) of [17] where  $P = x$ .  
 [35] M. Deserno, *Eur. Phys. J. E* **6**, 163 (2001).